Transmembrane Chloride Transport by Diphosphine–Pd(II) Complexes: Effect of the Ligand Geometry

Alessio Vidal, Massimo Tosolini, Gabriele Balducci and Paolo Tecilla*

Department of Chemical and Pharmaceutical Sciences, University of Trieste, Via Licio Giorgieri 1, 34127 Trieste, Italy. E-mail: ptecilla@units.it

Abstract

Transmembrane chloride transport is a fundamental biological process, and its impairment is at the origin of severe genetic diseases such as cystic fibrosis. Synthetic anion carriers able to transport chloride and other anions across biological membranes are considered as putative candidates for treating these syndromes. We have proposed diphosphine–Pd(II) complexes as a new class of anion carriers and in this contribution we have investigated the ionophoric activity of a family of Pd(II) complexes with diphosphine chelating ligands differing for the ligand bite angle that is varied from 71° (dppm) to 98° (dppb). Moreover, in the case of the dppe ligand we also investigated the effect of the introduction in the ligand structure of alkyl substituents of increasing length and hydrophobicity and of electron donor and withdrawing substituents. All the complexes investigated are able to transport chloride across the phospholipid membrane of liposomes and the most important parameter influencing their relative efficacy is the lipophilicity of the complex with the highest activity observed for [Pd(pEt-dppe)Cl_2]. On the contrary the bite angle of the ligand appears not relevant while the activity is diminished by the insertion of both EWG and EDG groups on the phenyl substituents of the phosphine ligands. Finally, also Ni(II) and Cu(I) complexes display ionophoric activity demonstrating that the transport ability of metal complexes is not limited to Pd(II) metal ion.

Introduction

Transmembrane chloride transport is a fundamental biological process which is normally regulated by complex membrane proteins, known as chloride channels (ClC). The impairment of these natural anion transporters has been associated with serious genetic diseases like cystic fibrosis and Bartter syndrome.[1] For this reason, the development of efficient synthetic anion transporters is receiving increasing attention[2] in the search of alternative therapies to treat these syndromes.[3,4] Moreover, anion transporters show interesting different biological properties,[5,6] in particular as antimicrobial[7,8] and anticancer agents.[9,10]

Most of the reported anionophores share as common elements a recognition site capable of efficiently recognize and coordinate anions through hydrogen bonding, embedded in a lipophilic scaffold that ensures partition in the phospholipid membrane.[2] Moreover, an increasing number of studies show that the most important parameters in determining anion transport efficiency are the affinity of the carrier for the transported anions[11,12,13,14,15] and the lipophilicity[11,16,17,18] of the molecules. In

particular, while the correlation between transport activity and binding constant for the anions is often complex and usually it does not seem to extend beyond closely related molecules, the effect of the lipophilicity of the carrier is more general and follows a bell-shaped correlation with an optimal value as a result of the compromise between the need to form a lipophilic complex able to cross the membrane and the need for the ionophore to approach the membrane/water interphase where the ion exchange process occurs.[19]

Due to the inherent ability of metal ions to coordinate anions[20] and to the ease modification of the organic ligand structure to modulate properties such as, for example, lipophilicity, metal-organic coordination complexes are promising candidates for developing anion carries. However, in the design of ion transport systems metal complexes have been mainly exploited as structural elements to self-assemble active ion channels or as regulatory switches to gate ion transport.[21] In fact, studies of metal complexes able to transport anions within their coordination sphere are rare and, apart from some reports of the transport of amino acids[22,23,24] and of HCl[25] across a bulk chloroform membrane, examples are essentially limited to the observation of ionophoric activity of a Pd(II) complex with a lipophilic ethylene diamine ligand,[26] to the transport of chloride by metalloporphyrins[27] and by a gold complex with a phosphazane ligand,[28] and to a recent example from the group of Gale of the uphill transport of hydroxide ion across unilamellar vesicles mediated by organoplatinum complexes.[29]

We have recently reported that simple Pd(II) complexes with chelating diphosphine ligands behave as anionophores across phospholipid membranes. [30,31] In particular, ([Pd(dppp)Cl_2], dppp = 1,3-bis(diphenylphosphino)propane), is able to efficiently promote anion transport in liposomes at low concentrations showing good selectivity toward chloride anion.[30] The complex acts as a carrier promoting an anion/OH^- antiport with the transported anions directly bound to the metal ion. Prompted by this result we decided to study more in depth this process investigating the effect of structural changes in the coordinating ligand on the ionophoric activity. Here we report the preparation and the investigation of the ionophoric activity of a family of Pd(II) complexes with diphosphine chelating ligands differing for the ligand bite angle that is varied from 71° (dppm) to 98° (dppb). In the case of the dppe ligand we also investigated the effect of the introduction in the ligand structure of alkyl substituents of increasing length and hydrophobicity and of electron donor and withdrawing substituents. Moreover, to broaden the scope of the work and to prove that transition metal complexes are efficient ionophores we investigated the transport abilities of metal complexes with metal ions different than Pd(II).

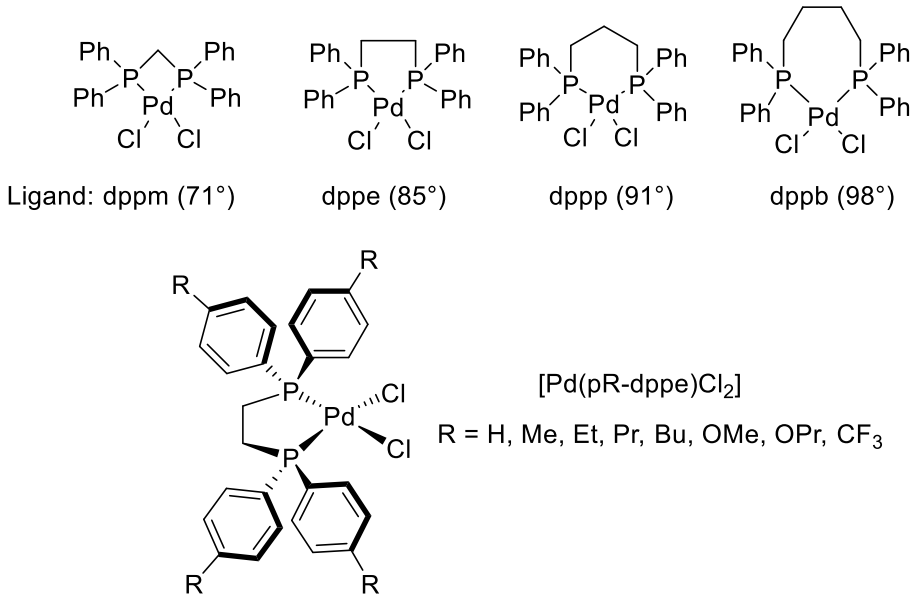

Figure 1. Structure of the Pd(II) diphosphine complexes investigated in this work. In brackets is reported the bite angle of the ligand.

Results and Discussion

Synthesis

Ligands dppm, dppe, dppp, and dppb are commercially available chelating diphosphines and have been chosen because, while maintaining the same substitution pattern on the two phosphorus atoms, are characterized by an increasing length of the methylene bridge connecting the two donor atoms. This results in a homogenous series of ligands differing in the ligand bite angle (Figure 1). The bite angle (β), defined as the P−M−P angles in diphosphine complexes, can have pronounced effects on the properties of the Pd(II) complexes for example influencing their efficiency and selectivity in various catalytic reactions due to steric and electronic effects.[32,33] With Pd(II) the ligands form square planar complexes[34] and represent a versatile tool to screen a series of closely related complexes having similar structure but different electronic and steric properties.

The ligand dppe was symmetrically modified by the introduction of substituents in the para position of the four phenyl rings in order to avoid steric perturbation of the chelating portion of the molecule. The substituents chosen were alkyl groups of increasing length from one to four carbon atoms, to explore complexes of different lipophilicity, and a trifluoromethyl and a methoxy or a propoxy group to have ligands with similar lipophilicity but different electronic properties. The synthesis of these derivatives started from the electrophilic reagent bis-(1,2-dichlorophosphino)ethane which is reacted with the Grignard reagent obtained from the properly substituted *p*-bromobenzene (Scheme 1).[35] This reaction yields directly the diphosphines which, however, being prone to oxidation in air are difficult to purify and store. To overcome this problem, the two phosphine groups were protected by complexation with borane. This protecting group has the advantage of being stable in air and in flash column chromatography, thus making easier the purification and storage of the products. Moreover, borane complexation is easily obtained by in-situ generation of BH_3 with sodium borohydride and

acetic acid in THF. In this way the protected phosphines were obtained with a yield in the range of 40-50%, depending on the R substituent. Once the borane-protected phosphines were obtained, the deprotection consisted simply in heating the molecule in methanol under microwave irradiation at 125°C.[36] This provides the free phosphine along with the boronic esters of methanol, which, being volatile, can be removed by simple evaporation. Finally, the Pd(II) complexes were obtained by reacting the diphosphine ligands with norbornadiene palladium dichloride complex as Pd(II) precursors in methanol. The ligand exchange takes place in few minutes and the target complex precipitates readily from the reaction mixture, yielding the pure complex with a yield in the range of 50 to 90%. The same procedure was used to prepare the Pd(II) complex of the non-functionalized ligands. All the complexes were fully characterized by ^{1}H- ,^{13}C- and ^{13}P-NMR, HSQC, HMBC, HH-COSY e NOESY 2D experiments and by ESI-MS.

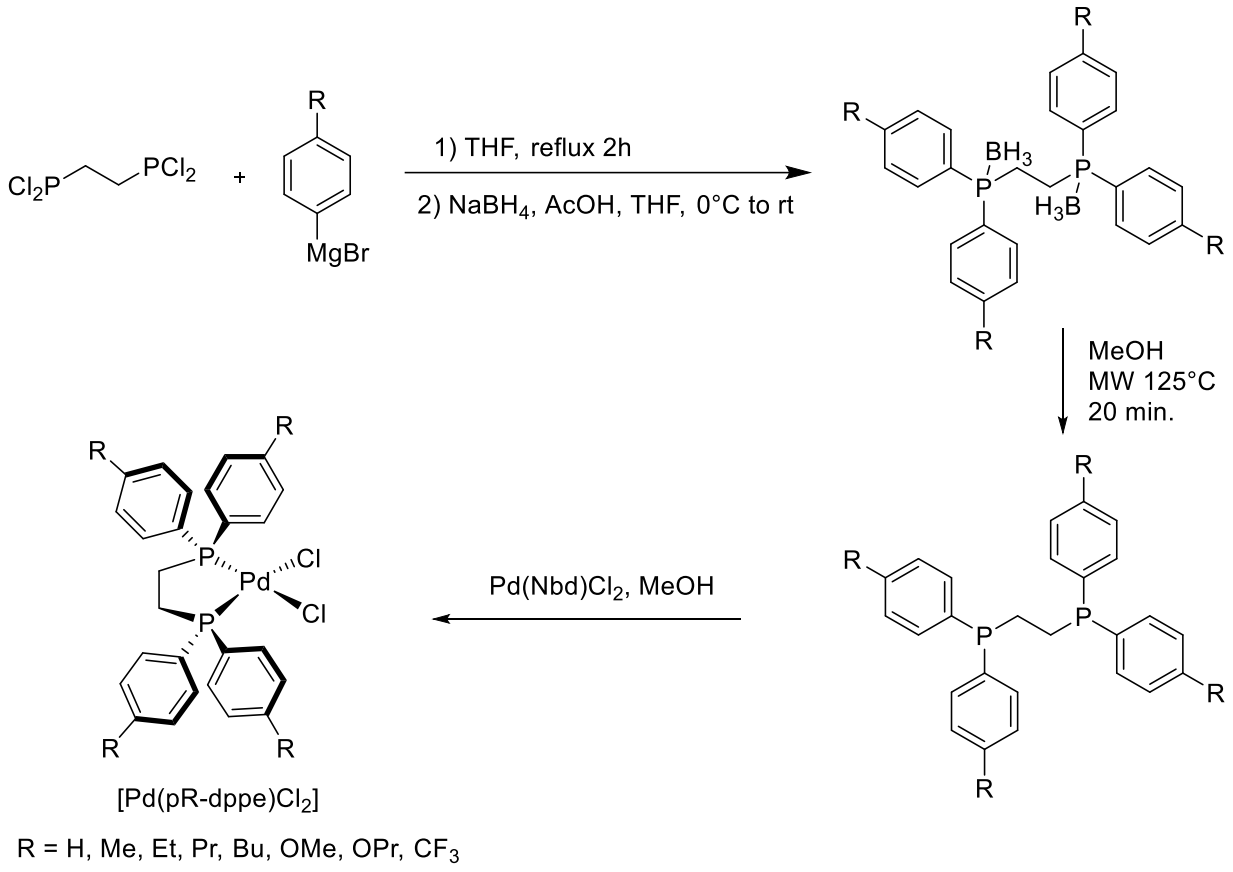

Scheme 1. Synthesis of the [Pd(pR-dppe)Cl_2] complexes.

The different reaction steps of Scheme 1 can be easily followed by ^{31}P-NMR as exemplified in Figure 2 in the case of the pMe-dppe derivative. In the diphosphine borane complex, the chemical shift of the phosphorus atoms is at ca. 15 ppm and the peak is broadened by the presence of the boron atom. Upon deprotection to diphosphine, the chemical shift is moved to higher fields, at around -15 ppm. Complexation to Pd(II) leads to a strong donation of charge from the phosphine to the palladium and, as a consequence, a strong downfield shift is observed with the phosphorus atoms of [Pd(pMe-dppe)Cl_2] that resonate at about 63 ppm.

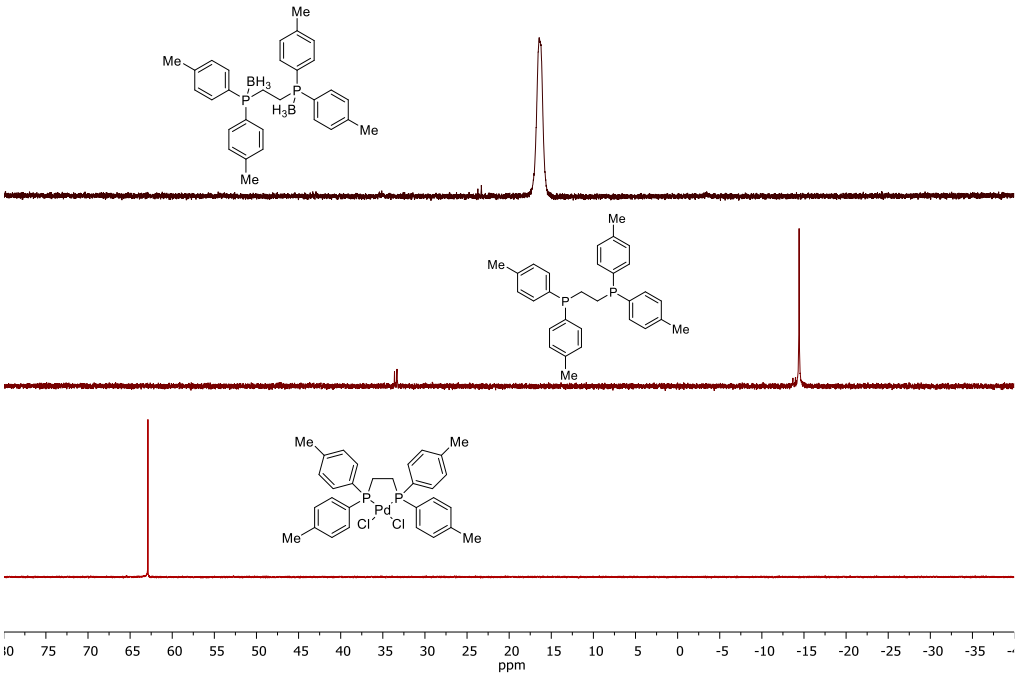

Figure 2. ^{31}P-NMR spectra of pMe-dppe-2·BH_3, pMe-dppe and [Pd(pMe-dppe)Cl_2] in $CDCl_3$.

In the case of [Pd(pMe-dppe)Cl_2], [Pd(pCF_3-dppe)Cl_2] and [Pd(pOMe-dppe)Cl_2] the structure of the complex was confirmed by single crystal X-ray diffraction analysis. Crystals of the complexes suitable for X-ray crystallography were obtained by slow evaporation from a CH_2Cl_2 solution. The molecular structure of the [Pd(pMe-dppe)Cl_2] is shown in Figure 3. Relevant interatomic bond lengths and bite angles are listed in Table 1 while the molecular structure of the other complexes and further crystallographic information are reported in the Supporting Information.

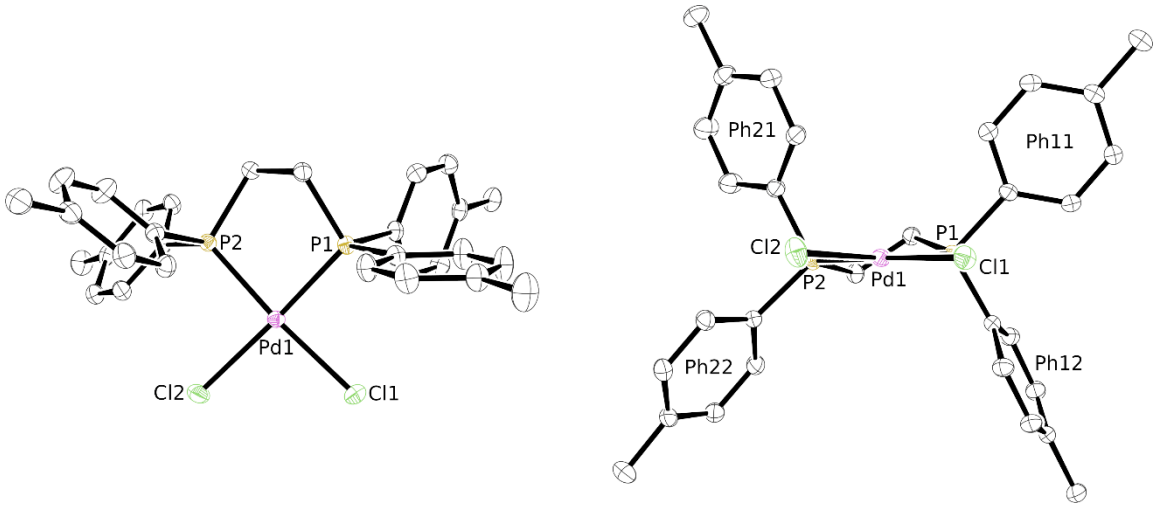

Figure 3. ORTEP representations (50% probability ellipsoids) of the molecule of complex [Pd(pMe-dppe)Cl_2] in the crystal structure; top view (left) and side view (right), with respect to the square coordination plane of the metal. For more clarity, hydrogen atoms have been omitted.

Table 1. Selected averaged[a] interatomic distances [Å] and bite angles [deg] for [Pd(pR-dppe)Cl_2] complexes.

Complex	Bite angle	Pd-P	Pd-Cl
[Pd(dppe)Cl_2][b]	85.8	2.230	2.359
[Pd(pMe-dppe)Cl_2]	86.5	2.238	2.354
[Pd(pCF_3-dppe)Cl_2]	85.9	2.248	2.359
[Pd(pOMe-dppe)Cl_2]	86.1	2.227	2.371

a) The Pd-P and the Pd-Cl distances reported are the average of the distances of the two phosphorus and chloride atoms from the metal ion; b) data from reference [34].

The different complexes show very similar molecular structures with the Pd(II) metal ion adopting in all cases a slightly distorted square planar geometry. As shown in Table 1, the introduction of EWG or EDG substituents on the phenyl rings has a negligible effect on the bite angle and on the lengths of the Pd-P and Pd-Cl bonds, with only the P-Cl bond in the [Pd(pOMe-dppe)Cl_2] complex marginally longer with respect to the other complexes

Ionophoric activity

The ionophoric activity of the complexes was investigated using liposomes as model for biological membranes and HPTS as a pH sensitive fluorescent probe. In a typical experiment, a suspension of unilamellar vesicles (lipid composition EYPC:EYPG 95:5, 100 nm in diameter) loaded with HPTS (8-hydroxypyrene-1,3,6-trisulfonic acid, 0.1 mM) were prepared in a buffered solution (25 mM HEPES, pH 7.0) containing 100 mM NaCl. The vesicles were suspended in an isotonic solution and the Pd(II) complexes solubilized in DMSO were added. Then a transmembrane pH gradient of ca. 0.6 pH units was established by external addition of NaOH. The resultant transport of OH^- inside the vesicles (or the kinetically equivalent H^+ efflux) was monitored measuring the increase in fluorescence emission of HPTS. At the end of the experiment, the vesicles were lysed by addition of detergent (Triton X-100) allowing to measure the maximal intensity of fluorescence which is then used to normalize the data (see Experimental section and Supporting Information for a more detailed description of the experiment).

Figure 4a reports the kinetic profiles recorded in the HPTS assay in the presence of increasing concentrations of the complex [Pd(dppm)Cl_2]. The kinetics traces were fitted with a first-order-rate equation to obtain the apparent rate constants for the transport process (k_t, s^{-1}), which are reported in Figure 4b. Similar results were obtained with the Pd(II) complexes of dppe, dppp, and dppb and are reported in Figure S2. With the exception of [Pd(dppe)Cl_2] the dependence of the ionophoric activity from the concentration of metal complex (Figure 4b and S2) is not linear but shows an upward curvature suggesting the participation of species of higher molecularity in the transport process. This behavior was already observed[30] with [Pd(dppp)Cl_2] and was attributed to the formation of dimeric

Pd–complexes, probably stabilized by μ-OH^- bridges.[37] The profiles were therefore fitted with the equation proposed by Regen that describes the formation of self-assembled active species,

$$k_t = k_2 K^{-1}[\text{Pdcomplex}]^n$$

where k_t is the observed kinetic constant, k_2 is the intrinsic rate constant of the transport process and K is the dissociation constant of the aggregate-monomer equilibrium involving *n* monomers.[38] The *n* values obtained range from 1.0 (dppe) to 2.82 (dppb) with the other two complexes showing intermediate values (1.73 for dppm and 1.70 for dppp). Therefore, in the case of [Pd(dppb)Cl_2] the participation of aggregate species in the transport process appears to be important while the low *n* values measured for the other complexes suggest a less relevant participation. In any case the formation of dimeric species is not surprising when considering that, although the analytical concentration of Pd(II) complexes in the kinetic experiments is in the range of 10^{-5} M, these complexes are poorly soluble in water and concentrate in the membrane increasing the local concentration of metal complexes and favoring aggregation processes.

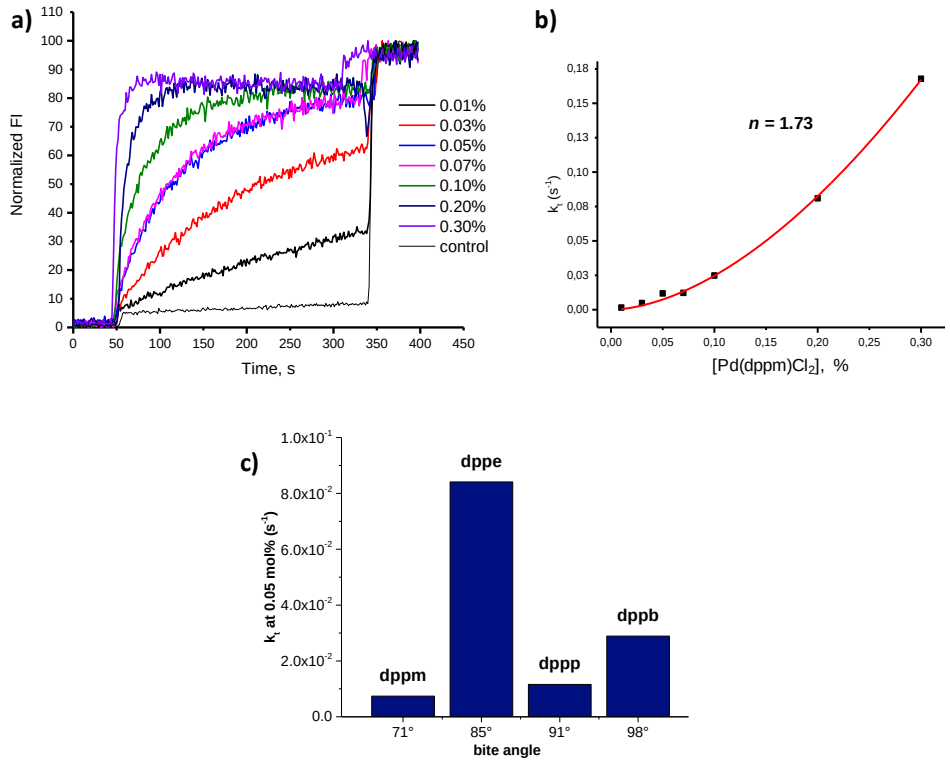

Figure 4. a) Normalized fluorescence changes in HPTS fluorescence emission (FI) as a function of time after addition of the base (50 μL of 0.5 M NaOH) to EYPC/EYPG LUVs (100 nm diameter) loaded with HPTS (0.1 mM HPTS, 0.17 mM total lipid concentration, 25 mM HEPES, 100 mM NaCl, pH 7.0, total volume 3 mL), in the presence of increasing concentration of [Pd(dppm)Cl_2] or in the absence of complex (control). The concentration of the metal complexes is given in % with respect to the total concentration of lipids. b) Dependence of the first order rate constant of the transport process (k_t, s^{-1}) on the concentration of [Pd(dppm)Cl_2]. The data has been fitted with the equation proposed by Regen. The *n* value obtained is reported in the graph. c) First order rate constants measured at 0.05 mol% ionophore concentration versus bite angle of the diphosphine ligand.

To compare the transport activity of the four complexes the first order rate constant measured at 0.05 mol% ionophore concentration was plotted against the bite angle of the ligands (Figure 4c). While the activities of the complexes with dppm, dppp and dppb are similar with an apparent small increase with the increase of the bite angle, [Pd(dppe)Cl_2] outperforms showing a much higher transport rate.

To investigate the parameters influencing the transport ability of the dppe complex we prepared and studied a family of dppe derivatives symmetrically functionalized in the *p*-position of the four phenyl rings with alkyl groups of increasing length and with electron withdrawing and electron donating substituents (Scheme 1). The ionophoric activity of the pR-dppe metal complexes was investigated using the HPTS assay and the kinetic profiles obtained at different ionophore concentrations are reported in Figure S3 with the exception of the pBu-dppePdCl_2 complex which is virtually inactive in the transport experiment (Figure S4). Also in this case, the activity/concentration profiles for the pR-dppe derivatives are not linear and show an upward curvature, with the exception of the non-substituted dppe. The *n* coefficients obtained from the Regen equation vary between 1 (R=H) and 1.75 (R=Pr), showing an apparent small increase associated with the increase of the lipophilicity of the ligand (Table S1). In any case, the absolute values of *n* are low indicating little participation of complexes with higher stoichiometry to the transport process. Figure 5 reports first order rate constants in the HPTS test measured at 0.05 mol% ionophore concentration versus the logP of the phospine oxide of the different ligands (pR-dppeOx) calculated with the software AClogP. The software and the phospine oxide were chosen because a good correlation between the logP calculated and experimentally determined by HPLC was found for a correlated family of diphosphine oxide compounds.[39] The values of logP calculated for the ligand oxides were used to describe the lipophilicity of the palladium complexes on the reasonable assumption that, being the $PdCl_2$ fragment identical in all the complexes, its effect on the lipophilicity would be the same for all the considered compounds.

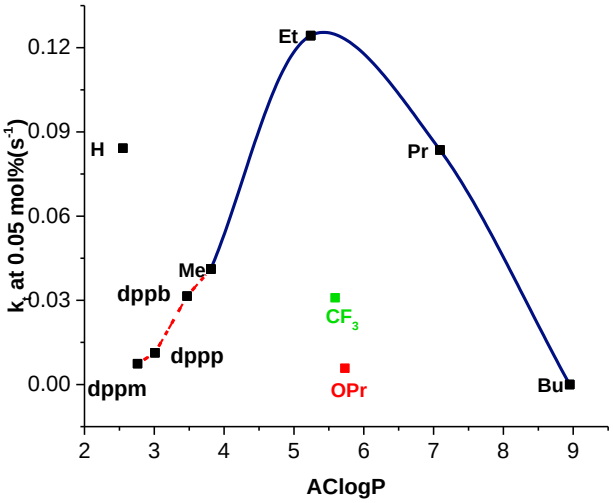

Figure 5. First order rate constants in the HPTS test (ionophore 0.05 mol%) versus calculated logP (AClogP) of pR-dppeOx (alkyl residues in black, CF_3 in green and OPr in red) and for dppm, dppp and dppb. The blue line is the correlation obtained with the alkyl series of [Pd(pR-dppe]Cl_2].

The data of Figure 5 show that the activity of the complexes bearing alkyl substituents follows a bell-shaped correlation with logP and the maximum activity is observed for [Pd(pEt-dppe)Cl_2] (blue line in Figure 5). This behavior is frequently observed for anion carriers and it is the result of the fact that too hydrophilic carriers are not able to solubilize in the membrane while too hydrophobic molecules are buried in the membrane and are not able to approach the surface where anion exchange takes place. It is interesting to not that also the non-substituted complexes of dppm, dppp and dppb ligands follow approximately the same correlation (red dotted line in Figure 5) suggesting that the different activity of these complexes is likely related to their lipophilicity instead of the different bite angle of the ligands. Surprisingly, the non-substituted dppe (R=H) was more active than expected from the correlation, evidencing that the introduction of the alkyl residue is detrimental for the activity. On the other hand, the introduction of both electron-donor (R = OPr) and withdrawing groups (R = CF_3) decreases the transport activity of the complexes which at parity of logP is much lower than that observed for [Pd(pEt-dppe)Cl_2]. This suggests a strong sensibility of pR-dppe complexes toward electronic effects and, considering that alkyl groups have a low but significant electron donor effect (Sigma Hammet for -CH_3: σ_p = -0.17 σ_p^+ = -0.31), this could explain the sharp decrease in activity found on moving from dppe to pMe-dppe.

Chloride binding in solution

Although the molecular structures determined in the solid state do not show relevant differences between the complexes, the ionophobic activity data suggest a strong influence of the electronic properties of the substituents on the transport activity. The substituents modify the electron density on the phosphines and therefore their donor ability toward the Pd(II). This is clearly seen by analyzing the chemical shifts of phosphorus in the complexes and in the free ligands. Substituted 1,3-bis(diarylphosphino)ethane derivatives have a typical ^{31}P-NMR resonance in the negative range, usually between -15/-20 ppm. Upon complexation with Pd(II), the electron density of the P-donor atom is transferred to the metal ion, resulting in a strong shift of the ^{31}P-NMR signal to around 60 ppm. The difference in chemical shift between the phosphorus signal in the free phosphine and in the Pd(II) complex, defined as $\Delta\delta$(ppm), is correlated to the amount of electronic density transferred from the P-donor to the metal ion and, therefore, to the strength of the interaction between phosphorus and the metal atom. Figure 6 reports the $\Delta\delta$ values for the different complexes, plotted against the σ_p or σ_p^+ Hammet's constants of the substituents. A good linear correlation with a negative slope is observed and, as expected, electron donating substituents increase the donation of electron density to Pd(II) resulting in higher $\Delta\delta$ values. On the other hand, electron withdrawing groups, have the opposite effect. Moreover, a better correlation is obtained using σ_p^+ indicating that the substituent is in direct interaction with the donor atom.

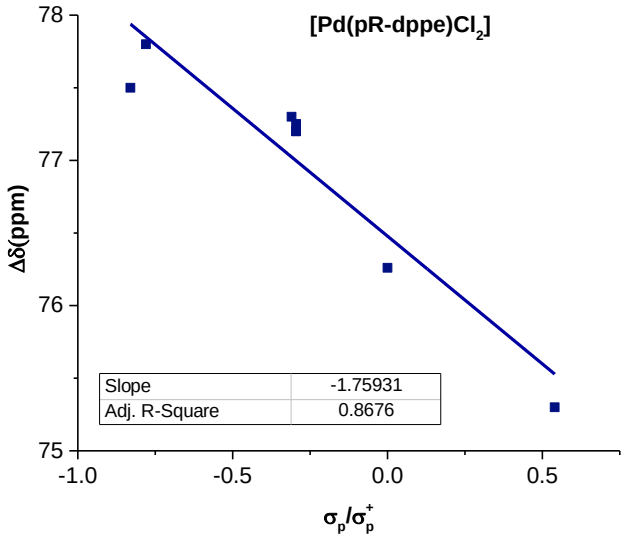

Figure 6. Hammett correlation between σ_p/ σ_p^+ and Δδ(ppm) of ^{31}P-NMR in $CDCl_3$. Δδ(ppm) is the difference in chemical shift between the phosphorous signal in the free phosphine and in the [Pd(pR-dppe)Cl_2] complexes.

Because substituents on the phenyl rings of the diphosphine ligand influence the electron donation toward the metal ion it is expected that they may also affect the strength of the Pd-Cl bond and in turn the ionophoric activity of the complexes. To verify this effect, we measured directly the association constant for chloride of a selection of complexes in a mixture of DMSO and water buffered with HEPES 25 mM at pH 7. Chloride atoms were first removed from the Pd(II) dichloride complexes by reaction with silver triflate and substituted with the less coordinating triflate anions. The resulting [Pd(pR-dppe)OTf_2] complexes were dissolved in DMSO/H_20 6:4 and titrated with NaCl following the evolution of the UV-Vis spectrum. In this conditions, however, [Pd(pCF_3-dppe)OTf_2] and [Pd(pOPr-dppe)OTf_2] precipitate during the titration hampering the determination of the association constants. For this reason we prepared the [Pd(pOMe-dppe)OTf_2] complex which being less lipophilic is more soluble in the solvent mixture. A typical titration experiment is reported in Figure S7 and shows an increase of absorbance at about 270 nm and a decrease at about 305 nm without any clear isosbestic point. The UV-Vis titration spectra were globally fitted to a 1:2 consecutive binding model using Bindfit. [40] The use of a local fitting approach, especially in case of a 1:2 binding model, can lead to great uncertainty on the determined K_a values, while a global fit of the whole UV-Vis spectra can greatly improve the accuracy of the fitted isotherms. [41] The titrations were repeated several times (Table S2-4) and the averaged values of the first (K_{a1}, M^{-1}) and of the second (K_{a2}, M^{-1}) chloride association constants together with the standard deviation are reported in Table 2.

Table 2. Averaged value of the first (K_{a1}, M^{-1}) and second (K_{a2}, M^{-1}) association constants of [Pd(pR-dppe)OTf_2] with chloride in DMSO/HEPES (25mM) 6:4 at 25 °C.

Complex	K_{a1} (M^{-1})	S.D.	K_{a2} (M^{-1})	S.D.
[Pd(dppe)OTf_2]	$9.2\cdot10^4$	$1.5\cdot10^4$	$2.52\cdot10^3$	$2.2\cdot10^2$
[Pd(pMe-dppe)OTf_2]	$6.69\cdot10^4$	$6.7\cdot10^3$	$2.02\cdot10^3$	$1.1\cdot10^2$
[Pd(pOMe-dppe)OTf_2]	$3.87\cdot10^5$	$4.6\cdot10^4$	$2.94\cdot10^3$	$3.2\cdot10^2$

As expected there is a significant influence of the substituents on the affinity constant of the complexes for chloride, although it appears that there is no simple correlation between the nature of the substituent and its effect on the K_a for chloride. Indeed, it is reasonable to assume that electron donating substituents increasing the electron density on Pd(II) should decrease the strength of the Pd-Cl bond and as consequence the association constant of the complex for the anion, and vice versa in the case of EWG substituents. Instead, a strong donor like the OMe group strongly increases K_{a1} with respect to the unsubstituted ligand while a weaker donor such as CH_3 has an opposite, although smaller, effect and the same trend is followed by K_{a2}. Therefore, the effect of the substituents on the phosphine ligands on the affinity of the palladium complexes toward chloride in solution is much more complex than expected, and the data obtained do not allow a correlation with the ionophoric activity of the complexes. In any case, in absolute values, the affinity constants measured for the different complexes are not much different and it is reasonable to assume that the effect on the transport activity is limited.

Anion selectivity and evidences for carrier mechanism

To better characterize the transport process anion selectivity was investigated using the NaX jump assay.[42] In this experiment the liposome suspension is prepared in a buffered solution in the absence of any NaX salt, with HPTS loaded in the inner water pool. Instead of creating a pH gradient using a NaOH pulse, the anion transport is induced with the rapid injection of an appropriate NaX solution. This creates a gradient of anions, which, in presence of an ionophore, is discharged by X^-/OH^- antiport leading to acidification of the liposome inner water pool that is signaled by the change in the fluorescence of HPTS. Since in all experiments the sodium salt of each anion is used, the relative rates observed using different anions give information on the selectivity of transport of anions (see Supporting Information for a more detailed description of the experiment). Figure 7a reports the normalized fluorescence intensity measured after 100 s from the NaX pulse and corrected for the anions permeation in the absence of ionophore using [Pd(dppe)Cl_2] [Pd(pOMe-dppe)Cl_2] and [Pd(pCF_3-dppe)Cl_2] as ionophores. Chloride and bromide are transported more efficiently than oxygenated anion, whereas the highly hydrophilic sulphate is essentially non-transported, with [Pd(pOMe-dppe)Cl_2] showing a slightly lower selectivity. These results, are in agreement with the findings reported previously for [Pd(dppp)Cl_2] and are related to the low affinity of oxygenated anion for Pd(II) complexes.[30] On the other hand, the inactivity observed in the case of sulfate is due to its

high hydrophilic character, which hinders the passage across the lipophilic environment of the phospholipid bilayer.

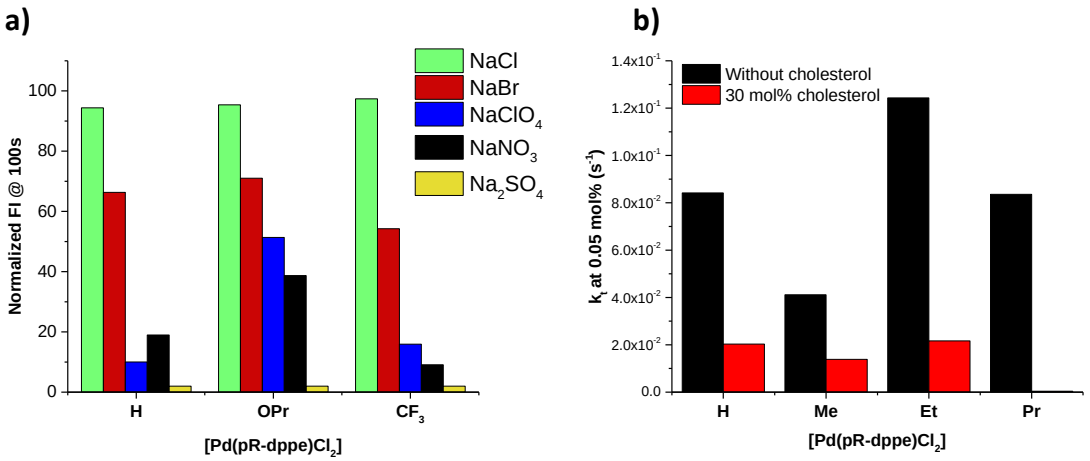

Figure 7. a) NaX jump anion selectivity test, normalized fluorescence intensity measured after 100 s from the NaX pulse and corrected for the background anion permeation in the presence of 0.1% concentration of [Pd(pR-dppe)Cl_2] (R = H, OPr, CF_3). b) First order rate constants in the HPTS test (ionophore 0.05 mol%) in the absence (black columns) and in the presence (red columns) of cholesterol 30 mol%; ionophore: [Pd(pR-dppe)Cl_2] (R = H, Me, Et, Pr).

To collect evidences on the mechanism of transport the ionophoric activity of the Pd(II) complexes was tested using liposomes containing cholesterol (lipid composition PC:PG:cholesterol 66.5:3.5:30). Cholesterol is known to decrease the fluidity of the membrane and it is used to discriminate transport mechanisms because, in a more rigid membrane environment, the activity of a mobile carrier is decreased while that of a channel system, which does not move in the membrane, should be unaffected.[43] In Figure 7b are reported the first-order rate constants (k_t, s^{-1}) for the transport process measured in the HPTS assay in the presence and in the absence of cholesterol (black and red columns, respectively) and using [Pd(pR-dppe)Cl_2] (R = H, Me, Et, Pr) as ionophores. The presence of the cholesterol in the membrane is associated with a significant decrease of activity, thus suggesting that Pd(II) based ionophores transport chloride with a mobile carrier mechanism.

Ionophoric activity of Ni(II) and Cu(I) dppe complexes

The studies reported so far involve only Pd(II) complexes. However, it was interesting to understand if the ability to transport anions is a prerogative of Pd(II) or is valid in general for other transition metals. Therefore, dppe complexes were prepared with Ni(II) and Cu(I). Figure 8 reports a comparison of the activity of the three complexes in the HPTS assay. Although with respect to [Pd(dppe)Cl_2] the Ni(II) and Cu(I) are less active they are both able to promote a measurable flux of anions with [Cu(dppe)Cl] being the most active. These findings are particularly interesting since they widen the scope of this research, suggesting that different metal ions could be used for anion transport

in liposomes. More studies are required and a careful screening of different type of ligands could, in principle, improve the ionophoric activity up to the level of Pd(II) complexes.

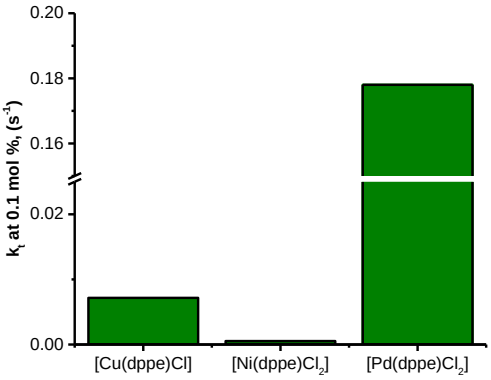

Figure 8. First order rate constants in the HPTS test in the presence of 0.1% concentration of [Pd(dppe)Cl_2], [Ni(dppe)Cl_2], and [Cu(dppe)Cl].

Conclusions

In the present work, we have investigated the ionophoric activity of a family of Pd(II) complexes with diphosphine chelating ligands. The results obtained show that all the complexes investigated are able to transport chloride across the phospholipid membrane of liposomes, although with different efficacy. Examining the effect of the different parameters on the activity of the complexes it appears that lipophilicity is the most relevant while the bite angle of the ligand is less important. On the other hand, the study has evidenced a high sensitivity of these systems to electronic effects with the [Pd(dppe)Cl_2] showing a high activity which, however, is detrimentally affected by the insertion of both EWG and EDG groups on the phenyl substituents of the phosphine ligands. This behavior was unexpected and requires further study to be better understood. Preliminary results have also shown that complexes with Ni(II) and Cu(I) as metal ions are active in the transport of anion. Overall, this study proved the general validity of the concept that transition metal complexes with diphosphine ligands are valid candidates for the development of anion transporters. Our further step is to widen to other complexes the structure activity relationship study to better understand the interplay of the different parameters influencing activity and to better define the mechanism of action of these systems. Moreover, the study of the biological activity of this class of complexes is underway.

Experimental section

Materials and general methods

The reagents and solvents have been purchased from Sigma-Aldrich or Alfa Aesar and used without further purification. Column chromatography was performed on silica gel 60 (Merck, 230–400 mesh ASTM), eluting with solvents mixtures as specified below. The reactions were monitored by TLC (silica gel/ UV 254, 0.20 mm, glass or aluminum support). UV-Vis spectra were recorded on an

Agilent Cary 60 spectrometer in a quartz cuvette (1 cm optic path length). Fluorescence emission spectra and kinetics were recorded on a Varian Cary Eclypse spectrofluorometer in a quartz cuvette (1 cm optic path length). Data collections for X-Ray structure determination were performed at the X-ray diffraction beamline (XRD1) of the Elettra Synchrotron, Trieste (Italy). Supplementary crystallographic data for this paper can be obtained free of charge from the Cambridge Crystallographic Data Centre using the following deposit numbers: 2209080 ([Pd(pCF$_3$-dppe)Cl$_2$]), 2209081 ([Pd(pOMe-dppe)Cl$_2$]), 2209082 ([Pd(pMe-dppe)Cl$_2$]). Mass spectra have been acquired using a Bruker Esquire 4000 ESI-MS instrument or a Bruker micrOTOF-Q for HRMS by Dr. Fabio Hollan. Only molecular ions and major peaks are reported. NMR spectra were recorded on a Varian 500 MHz (125 MHz for carbon and 202 MHz for phosphorous) or a Varian 400 MHz (101 MHz for carbon and 162 MHz for phosphorous). Chemical shifts are reported as parts per million (ppm) relative to the solvent residual signal as internal reference. Coupling constants (J) are quoted in Hertz (Hz). The s, d, t, q, quint, sex, m, and bs signal notations indicate respectively: singlet, doublet, triplet, quartet, quintet, sextet, multiplet and broad signal. All reagents were purchased from Sigma-Aldrich. 1-Bromo-4-propoxybenzene[44], [Pd(dppm)Cl$_2$][34], [Pd(dppe)Cl$_2$][34], [Pd(dppe)OTf$_2$][45], [Pd(dppp)Cl$_2$][30], [Pd(dppb)Cl$_2$],[46] [Ni(dppe)Cl$_2$],[47] [Cu(dppe)Cl][48] were prepared according to published literature.

General procedure for the synthesis of pR-dppe-2·BH$_3$ protected diphosphine ligands

In a round bottom flask, an appropriate amount of magnesium turnings (5 eq.) was dried by stirring under elevated temperature in Ar atmosphere. Dry THF was added together with a small amount of iodine. After stirring for 10 minutes, a proper amount of 1-bromo-4-R-benzene (4.7 eq.) was added dissolved in THF (ca. 0.5 M). The solution was refluxed for 2 hours. The Grignard solution was then cooled at room temperature and 1 eq. of 1,2-bis(dichlorophosphino)ethane was added with a syringe. After 2 hours under reflux the reaction was quenched with water and extracted with Et$_2$O three times. The organic phase was washed two times with NH$_4$Cl 5%, dried over Na$_2$SO$_4$, filtered and the solvent was removed under vacuum. The crude product was dissolved in dry THF in Ar atmosphere and NaBH$_4$ (3eq.) was added. The solution was cooled at 0°C using an ice bath and an excess of acetic acid was added dropwise. The solution was stirred at ambient temperature and the reaction was monitored by TLC (EP:DCM 3:7). After the reaction was complete, a solution of NaHSO$_4$ 5% was added and the reaction mixture was extracted three times with AcOEt. The organic phase was washed two times with NH$_4$Cl 5%, dried with Na$_2$SO$_4$, filtered and the solvent was removed under vacuum. The crude product was purified by flash column chromatography (EP:AcOEt), yielding the product as a white solid. ·

pMe-dppe-2·BH$_3$: 182 mg (MW=482.20 g/mol, 0.38 mmol, yield 38%). ESI-MS (m/z): 521.2 [M+K]$^+$, R$_f$=0.17 (EP:DCM 6:4); ^{1}H-NMR (400 MHz, CDCl$_3$) δ: 7.71-7.41 (m, 8H), 7.33-7.15 (m, 8H), 2.38 (s, 12H), 2.32 (d, 8H, J=7.0 Hz), 1.55-0.31 (bs, 6H); ^{13}C-NMR (101 MHz, CDCl$_3$) δ: 141.9, 132.2, 132.1, 132.0, 129.8, 129.8, 129.7, 125.2, 124.6, 21.4, 19.8, 19.4; ^{31}P-NMR (162 MHz, CDCl$_3$) δ: 16.4.

pEt-dppe-2·BH$_3$: 323 mg (MW=538.31 g/mol, 0.60 mmol, yield 50%). ESI-MS (m/z): 561.4 $[M+Na]^+$, 577.3 $[M+K]^+$, R_f=0.46 (EP:DCM 6:4); ^{1}H-NMR (400 MHz, $CDCl_3$) δ: 7.56 (m, 8H), 7.31-7.19 (m, 8H), 2.66 (q, J=7.6 Hz, 8H), 2.34 (m, 4H), 1.24 (t, J=7.6 Hz, 12H), 1.50-0.50 (bs, 6H); ^{13}C-NMR (101 MHz, $CDCl_3$) δ: 148.0, 132.3, 132.2, 132.1, 128.7, 128.6, 128.5, 125.4, 124.9, 77.3, 77.0, 76.7, 28.7, 19.8, 19.4, 15.1; ^{31}P-NMR (162 MHz, $CDCl_3$) δ: 16.1.

pPr-dppe-2·BH$_3$: 321 mg (MW=594.42 g/mol, 0.54 mmol, yield 47%). ESI-MS (m/z): 617.4 $[M+Na]^+$, R_f=0.60 (EP:DCM 6:4); ^{1}H-NMR (400 MHz, $CDCl_3$) δ: 7.55 (m, 8H), 7.23 (m, 8H), 2.60 (t, J=7.8 Hz, 8H), 2.35 (d, 4H, J=3.1 Hz), 1.63 (sex, J=7.6 Hz, 8H), 1.48-0.37 (bs, 6H), 0.94 (t, J=7.3 Hz, 12H); ^{13}C-NMR (101 MHz, $CDCl_3$) δ: 171.0, 146.6, 146.5, 146.4, 132.2, 132.1, 132.0, 129.2, 129.1, 129.0, 125.5, 124.9, 37.9, 24.2, 19.9, 19.5, 13.8; ^{31}P-NMR (162 MHz, $CDCl_3$) δ: 16.1.

pBu-dppe-2·BH$_3$: 323 mg (MW=650.53 g/mol, 0.49 mmol, yield 50%). ESI-MS (m/z): 673.4 $[M+Na]^+$, 689.4 $[M+K]^+$, R_f=0.60 (EP:DCM 6:4); ^{1}H-NMR (400 MHz, $CDCl_3$) δ: 7.56 (m, 8H), 7.25 (m, 8H), 2.63 (t, J=7.6 Hz, 4H), 2.36 (d, J=3.0 Hz, 4H), 1.60 (p, J=7.6 Hz, 8H), 1.36 (sex, J=7.4 Hz, 8H), 1.20-0.43 (bs, 6H), 0.93 (t, J=7.3 Hz, 12H); ^{13}C-NMR (101 MHz, $CDCl_3$) δ:146.8, 132.2, 132.1, 132.0, 129.2, 129.1, 129.0, 125.4, 124.8, 35.5, 33.2, 22.3, 19.9, 19.5, 13.9; ^{31}P-NMR (162 MHz, $CDCl_3$) δ: 16.2.

pOMe-dppe-2·BH$_3$: 466 mg (MW=546.20 g/mol, 0.85 mmol, yield 43%). ESI-MS (m/z): 569.2 $[M+Na]^+$; ^{1}H-NMR (400 MHz, $CDCl_3$) δ: 7.55 (m, 8H), 6.93 (m, 8H), 3.81 (s, 12H), 2.27 (d, 4H, J=3.1 Hz), 1.46-0.33 (bs, 6H); ^{13}C-NMR (101 MHz, $CDCl_3$) δ: 162.1, 133.8, 133.7, 119.6, 119.0, 114.7, 114.6, 114.5, 55.4, 20.3, 19.9,^{31}P-NMR (162 MHz, $CDCl_3$) δ: 14.9.

pOPr-dppe-2·BH$_3$: 354 mg (MW=658.41 g/mol, 0.54 mmol, yield 54%). ESI-MS (m/z): 681.4 $[M+Na]^+$, 689.4 $[M+K]^+$; ^{1}H-NMR (400 MHz, $CDCl_3$) δ: 7.53 (m, 8H), 6.92 (m, 8H), 3.92 (t, J=6.5 Hz, 8H), 2.27 (s, 4H, J=3.0 Hz), 1.80 (sex, J=7.0 Hz, 8H), 1.45-0.65 (bs, 6H), 1.02 (t, J=7.3 Hz, 12H); ^{13}C-NMR (101 MHz, $CDCl_3$) δ:161.6, 133.8, 133.7, 133.6, 115.2, 115.1, 115.00, 114.0, 113.9, 69.6, 22.4, 20.3, 19.9, 10.4; ^{31}P-NMR (162 MHz, $CDCl_3$) δ: 14.8.

pCF$_3$-dppe-2·BH$_3$: 237 mg (MW=698.09 g/mol, 0.34 mmol, yield 41%). ^{1}H-NMR (400 MHz, $CDCl_3$) δ: 7.82-7.71 (m, 16H), 2.44 (d, J=3.1 Hz, 4H), 1.41-0.43 (bs, 6H); ^{13}C-NMR (101 MHz, $CDCl_3$) δ:134.6, 134.3, 133.9, 133.6, 132.7, 132.6, 132.5, 131.8, 131.3, 127.2, 126.2, 124.5, 121.8, 119.1, 19.2, 19.1, 18.8; ^{31}P-NMR (162 MHz, $CDCl_3$) δ: 19.8; ^{19}F-NMR (376 MHz, $CDCl_3$) δ: -63.4

General procedure for the borane deprotection, synthesis of the pR-dppe diphosphine ligands

In a microwave vial, 0.15 mmol of pR-dppe-2BH_3 was dissolved in 5 mL of MeOH. The suspension was heated in the microwave at 125°C for 20 minutes. After checking the complete conversion of the starting material by TLC (EP:DCM 3:7), the solvent was removed under vacuum yielding a transparent oil. The phosphines were obtained in quantitative yield and were used immediately without further purification.

pMe-dppe: (MW=454.53 g/mol). R_f=0.33 (EP:DCM 7:3); ^{1}H-NMR (400 MHz, $CDCl_3$) δ: 7.21 (m, 8H), 7.12 (m, 8H), 2.33 (s, 12H), 2.04 (s, 4H); ^{13}C-NMR (101 MHz, $CDCl_3$) δ: 138.5, 134.8, 132.7, 129.1, 23.9, 21.2; ^{31}P-NMR (162 MHz, $CDCl_3$) δ: -14.4.

pEt-dppe: (MW=510.64 g/mol). R_f=0.59 (EP:DCM 6:4); ^{1}H-NMR (400 MHz, $CDCl_3$) δ: 7.28-7.25 (m, 8H), 7.17-7.07 (m, 8H), 2.63 (q, J=7.6 Hz, 8H), 2.12 (m, 4H), 1.22 (t, J=7.6 Hz, 12H); ^{13}C-NMR (101 MHz, $CDCl_3$) δ: 144.7, 135.0, 132.8, 127.9, 28.6, 23.9, 15.3; ^{31}P-NMR (162 MHz, $CDCl_3$) δ: -14.3

pPr-dppe: (MW=566.75 g/mol). R_f=0.61 (EP:DCM 6:4); ^{1}H-NMR (400 MHz, $CDCl_3$) δ: 7.29-7.24 (m, 8H), 7.11 (m, 8H), 2.56 (t, J=7.6 Hz, 8H), 2.08 (s, 4H), 1.62 (sex, J=7.4 Hz, 8H), 0.93 (t, J=7.3 Hz, 12H); ^{13}C-NMR (101 MHz, $CDCl_3$) δ: 43.2, 134.9, 132.6, 128.5, 37.8, 24.3, 24.0, 13.8; ^{31}P-NMR (162 MHz, $CDCl_3$) δ: -14.2

pBu-dppe: (MW=622.86 g/mol) transparent oil. R_f=0.35 (EP:DCM 7:3); ^{1}H-NMR (400 MHz, $CDCl_3$) δ: 7.28-7.21 (m, 8H), 7.18-7.05 (m, 8H), 2.59 (t, J=7.8 Hz, 8H), 2.06 (s, 4H), 1.59 (p, J=7.6 Hz, 8H), 1.35 (sex, J=7.4 Hz, 8H), 0.93 (t, J=7.3 Hz, 12H); ^{13}C-NMR (101 MHz, $CDCl_3$) δ: 143.4, 134.9, 132.6, 128.7, 35.4, 33.4, 24.0, 22.3, 13.9; ^{31}P-NMR (162 MHz, $CDCl_3$) δ: -14.3

pOMe-dppe: (MW=518.53 g/mol). R_f=0.37 (EP:DCM 3:7); ^{1}H-NMR (400 MHz, $CDCl_3$) δ: 7.28 (m, 8H), 6.86 (m, 8H), 3.81 (s, 12H), 2.01 (m, 4H); ^{13}C-NMR (101 MHz, $CDCl_3$) δ: 160.0, 134.1, 134.0, 133.9, 132.6, 132.5, 114.0, 55.1, 24.3; ^{31}P-NMR (162 MHz, $CDCl_3$) δ: -16.1.

pOPr-dppe: (MW=630.75 g/mol). R_f=0.66 (EP:DCM 3:7); ^{1}H-NMR (400 MHz, $CDCl_3$) δ: 7.25 (m, 8H), 6.84 (m, 8H), 3.90 (t, J=6.6 Hz, 8H), 2.00 (m, 4Hz), 1.80 (dt, J=6.6 Hz, J=7.4 Hz, 8H), 1.03 (t, J=7.4 Hz, 12H); ^{13}C-NMR (101 MHz, $CDCl_3$) δ: 159.6, 134.1, 134.0, 133.9, 129.2, 129.1, 129.0, 114.7, 114.6, 114.5, 69.3, 24.5, 24.4, 22.5, 10.5; ^{31}P-NMR (162 MHz, $CDCl_3$) δ: -16.0.

pCF$_3$-dppe: (MW=670.42 g/mol). R_f=0.38 (EP:DCM 7:3); ^{1}H-NMR (400 MHz, $CDCl_3$) δ: 7.57 (m, 8H), 7.40 (m, 8H), 2.13 (m, 4H); ^{13}C-NMR (101 MHz, $CDCl_3$) δ: 141.9, 132.9, 131.8, 131.4, 131.1, 130.8, 127.8, 125.5, 125.4, 125.1, 122.4, 119.7, 23.4; ^{31}P-NMR (162 MHz, $CDCl_3$) δ: -13.0; ^{19}F-NMR (376 MHz, $CDCl_3$) δ: -63.0.

General procedure for the synthesis of the [Pd(pR-dppe)Cl$_2$] complexes

[Pd(nbd)Cl_2] (0.9 eq) was added to a suspension of the appropriate pR-dppe ligand in dry MeOH. The yellow suspension cleared in a few minutes. The reaction mixture was stirred at ambient temperature overnight. An abundant precipitate was formed. The volume of the solvent was partially reduced under vacuum and Et_2O was added to promote precipitation at 5 °C. The suspension was then filtered and the solid was washed with cold Et_2O affording pure [Pd(pR-dppe)Cl_2] complexes.

[Pd(pMe-dppe)Cl$_2$]: 59 mg (MW=631.85 g/mol, 0.094 mmol, yield 70%) as light pale yellow solid. ESI-MS (m/z): 595.1 [M[Pd(II)]-Cl]$^+$; ^{1}H-NMR (400 MHz, $CDCl_3$) δ: 7.74 (m, 8H), 7.26 (m, 8H), 2.39 (s, 12H), 2.36 (m, 4H); ^{13}C-NMR (101 MHz, $CDCl_3$) δ: 142.7, 133.6, 133.5, 133.4, 129.9, 129.8, 129.7, 125.1, 124.5, 28.5, 28.0, 21.5; ^{31}P-NMR (162 MHz, $CDCl_3$) δ: 62.9.

[Pd(pEt-dppe)Cl$_2$]: 59 mg (MW=687.96 g/mol, 0.086 mmol, yield 65%) as light pale yellow solid. ESI-MS (m/z): 690.18 [M[Pd(I)]-Cl+K]$^+$; ^{1}H-NMR (400 MHz, $CDCl_3$) δ: 7.77 (m, 8H), 7.28 (m, 8H),

2.68 (q, J=7.5 Hz, 8H), 2.38 (m, 4H), 1.25 (t, J=7.6 Hz, 12H); ^{13}C-NMR (101 MHz, $CDCl_3$) δ: 148.7, 133.8, 133.7, 133.6, 128.7, 128.6, 128.5, 125.3, 124.8, 28.8, 28.6, 28.1, 15.0; ^{31}P-NMR (162 MHz, $CDCl_3$) δ: 62.9.

[Pd(pPr-dppe)Cl$_2$]: 50 mg (MW=744.07 g/mol, 0.067 mmol, yield 55%) as light pale yellow solid. ESI-MS (m/z): 673.3 [M[Pd(II)]-Cl]$^+$, 703.3 [M[Pd(0)]-2Cl+H]$^+$; ^{1}H-NMR (400 MHz, $CDCl_3$) δ: 7.76 (m, 8H), 7.26 (m, 8H), 2.61 (t, J=7.6 Hz, 8H), 2.38 (m, 4H), 1.65 (sex, J=7.6 Hz, 8H), 0.95 (t, J=7.3 Hz, 12H); ^{13}C-NMR (101 MHz, $CDCl_3$) δ: 147.3, 133.6, 133.5, 133.4, 129.3, 129.2, 129.1, 125.3, 124.8, 37.9, 28.6, 28.1, 24.1, 13.8; ^{31}P-NMR (162 MHz, $CDCl_3$) δ: 63.0.

[Pd(pBu-dppe)Cl$_2$]: 42 mg (MW=800.18 g/mol, 0.053 mmol, yield 45%) as light pale yellow solid. ESI-MS (m/z): 729.4 [M[Pd(II)]-Cl]$^+$; ^{1}H-NMR (400 MHz, $CDCl_3$) δ: 7.75 (m, 8H), 7.26 (m, 8H), 2.64 (t, J=7.6 Hz, 8H), 2.38 (m, 4H), 1.65-1.55 (m, 8H), 1.36 (sex, J=7.4 Hz, 8H), 0.93 (t, J=7.3 Hz, 12H); ^{13}C-NMR (101 MHz, $CDCl_3$) δ: 147.5, 133.7, 133.6, 133.5, 129.2, 129.1, 129.0, 125.3, 124.7, 35.6, 33.1, 28.6, 28.1, 22.3, 13.8; ^{31}P-NMR (162 MHz, $CDCl_3$) δ: 63.0.

[Pd(pOMe-dppe)Cl$_2$]: 140 mg (MW=695.85 g/mol, 0.20 mmol, yield 83%) as light pale yellow solid. ESI-MS (m/z): 659.1 [M[Pd(II)]-Cl]$^+$; ^{1}H-NMR (400 MHz, $CDCl_3$) δ: 7.77 (m, 8H), 6.95 (m, 8H), 3.83 (s, 12H), 2.33 (m, 4H); ^{13}C-NMR (101 MHz, $CDCl_3$) δ: 162.5, 135.4, 135.3, 135.2, 119.5, 119.4, 118.8, 118.7, 114.8, 114.7, 114.6, 55.4, 28.4, 27.9; ^{31}P-NMR (162 MHz, $CDCl_3$) δ: 61.7.

[Pd(pOPr-dppe)Cl$_2$]: 62 mg (MW=808.07 g/mol, 0.077 mmol, yield 67%) as light pale yellow solid. ESI-MS (m/z): 771.2 [M[Pd(II)]-Cl]$^+$, 831.2 [M[Pd(II)]+Na]$^+$; ^{1}H-NMR (400 MHz, $CDCl_3$) δ: 7.76 (m, 8H), 6.95 (m, 8H), 3.95 (t, J=6.5 Hz, 8H), 2.31 (m, 4H), 1.82 (sex, J=7.1 Hz, 8H), 1.04 (t, J=7.4 Hz, 12H); ^{13}C-NMR (101 MHz, $CDCl_3$) δ: 162.1, 135.3, 135.2, 135.1, 119.1, 118.5, 115.2, 115.1, 115.0, 69.6, 28.4, 27.9, 22.4, 10.4; ^{31}P-NMR (162 MHz, $CDCl_3$) δ: 61.5.

[Pd(pCF$_3$-dppe)Cl$_2$]: 81 mg (MW=847.74 g/mol, 0.096 mmol, yield 76%) as light pale yellow solid. ESI-MS (m/z): 870.9 [M[Pd(II)]+DMSO+H]$^+$; ^{1}H-NMR (400 MHz, $CDCl_3$) δ: 7.59-7.53 (m, 8H), 7.43-7.34 (m, 8H), 2.13 (s, 4H); ^{13}C-NMR (101 MHz, $CDCl_3$) δ: 134.5, 134.4, 134.3, 133.5, 133.2, 132.2, 131.7, 127.9, 125.8, 125.7, 125.6, 125.1, 122.4, 119.6, 28.2, 27.7; ^{31}P-NMR (162 MHz, $CDCl_3$) δ: 62.3; ^{19}F-NMR (376 MHz, $CDCl_3$) δ: -64.3.

General procedure for the synthesis of the [Pd(pR-dppe)OTf$_2$]

To a solution of the appropriate [Pd(pR-dppe)Cl_2] in dry DCM, 2.1 eq. of silver triflate were added. The reaction mixture was stirred at ambient temperature for 3 hours shielded from light. An abundant precipitate of AgCl was formed. The suspension was filtered through celite and Et_2O was added in order to promote the precipitation of a yellow solid. The solid was filtered yielding the pure di-triflate complex.

[Pd(pMe-dppe)OTf$_2$]: 105 mg (MW=859.08 g/mol, 0.12 mmol, yield 87%) as yellow solid. ^{1}H-NMR (400 MHz, $CDCl_3$) δ: 7.69-7.54 (m, 8H), 7.42-7.31 (m, 8H), 2.69-2.51 (m, 4H), 2.42 (s, 12H); ^{13}C-NMR (101 MHz, $CDCl_3$) δ: 145.1, 133.1, 133.0, 130.9, 130.8, 124.6, 121.4, 120.9, 120.3, 118.3, 115.1, 27.3, 27.2, 26.9, 26.8, 21.7; ^{31}P-NMR (162 MHz, $CDCl_3$) δ: 71.5.

[Pd(pOMe-dppe)OTf$_2$]: 104 mg (MW=923.08 g/mol, 0.11 mmol, yield 75%) as yellow solid. ^{1}H-NMR (400 MHz, $CDCl_3$) δ: 7.72-7.59 (m, 8H), 7.09-6.99 (m, 8H), 3.86 (s, 12H), 2.65-2.41 (m, 4H); ^{13}C-NMR (101 MHz, $CDCl_3$) δ: 163.9, 134.9, 134.8, 124.7, 121.5, 118.4, 115.8, 115.7, 114.9, 114.2, 113.7, 55.6, 27.4, 27.0; ^{31}P-NMR (162 MHz, $CDCl_3$) δ: 69.9.

Ion transport studies

General procedures. L-α-phosphatidyl-DL-glycerol sodium salt (EYPG, 20 mg/mL chloroform solution) was purchased from *Avanti Polar Lipids*, egg yolk phosphatidylcholine (EYPC, 100 mg/mL chloroform solution), lucigenin and 8-hydroxypyrene-1,3,6-trisulfonic acid trisodium salt (HPTS) were from *Sigma*; Triton® X-100 and HEPES (4-(2-hydroxyethyl)1-piperizine ethanesulfonic acid) were from *Fluka*; all salts were of the best grade available from *Aldrich* and were used without further purification. Size exclusion chromatography (SEC) was performed using Sephadex™ G-75 or pre-packed columns Sephadex™ G-25 M (PD-10) from *Amersham Biosciences*. Liposome were prepared by extrusion using a 10 mL Lipex™ Thermobarrel EXTRUDER (Northern Lipids Inc.) connected to a thermostatic bath (25°C). The 100 nm polycarbonate membranes are Nucleopore track-Etch Membranes from *Whatman*. Fluorescence spectra were recorded on Varian Cary Eclipse fluorimeter. All fluorimetric experiments were conducted at 25°C. The ionophores concentration is given in percent with respect to the total concentration of lipid. Mother solutions of ionophores were prepared in DMSO or in MeCN. Control experiments showed that the amount of solvent added to the vesicular suspension in the different experiments (maximum amount 2.00% in volume) did not affect membrane permeability. The logP values of the compounds were calculated using the ALOGPs 2.1 software (VCCLAB, V.C.C.L., http://www.vcclab.org).

HPTS assay. 150 μL of EYPC chloroform solution (100 mg/mL, 20 μmol) and 40 μL of EYPG chloroform solution (20 mg/mL, 1.0 μmol) was first evaporated under Ar-flux to form a thin film and then dried under high vacuum for 3 h. If required, 66 μL of cholesterol chloroform solution (50 mg/mL, 8.5 μmol) were added. The lipid cake was hydrated in 1.5 mL of 0.1 mM HPTS solution (25 mM HEPES, 100 mM NaCl, pH 7) for 30 min at 40 °C. The lipid suspension was subjected to five freeze–thaw cycles (−196 °C/40 °C) using liquid nitrogen and a thermostatic bath, and then extruded under nitrogen pressure (15 bar) at room temperature (10 extrusions through a 0.1 μm polycarbonate membrane). The LUV suspension was separated from the extravesicular dye by size exclusion chromatography (SEC) (stationary phase: pre-packed column Sephadex™ G-25, mobile phase: 25 mM HEPES buffer, 100 mM NaCl, pH 7) and diluted with HEPES buffer (25 mM HEPES, 100 mM NaCl, pH 7) to give a stock solution with a lipid concentration of 5 mM (assuming 100% of lipids were incorporated into liposomes). 104 μL of the lipid suspension were placed in a fluorimetric cell and diluted to 3040 μL with the same buffer solution. The total lipid concentration in the fluorimetric cell was 0.17 mM. An aliquot of the solution of the ionophore in MeOH or DMSO (10–60 μL of the appropriate mother solution in order to obtain the desired $mol_{compound}/mol_{lipid}$ ratio) was then added to the lipid suspension and the cell was incubated at 25 °C for 10 min. After incubation, the time course of fluorescence was recorded for 50 s monitoring the HPTS emission at 510 nm with excitation wavelengths set alternately at 403 and 460 nm on a 0.5 + 0.5 s cycle. Then 50 μL of 0.5 M NaOH were rapidly added through an injector port and the fluorescence emission was recorded for 350 s.

Maximal changes in dye emission were obtained by the final lysis of the liposomes with a detergent (40 μL of 5% aqueous Triton® X-100). The data set consists of emission intensities at 510 nm modulated by alternating excitation at 403 nm and 460 nm on a 0.5 + 0.5 s cycle. The concentration of the conjugate base form of HPTS is related to the emission intensity at 510 nm during the period in which the dye is excited at 460 nm (E460) while the concentration of the protonated form is related to the emission intensity at 510 nm during the period in which the dye is excited at 403 nm (E403). Fluorescence time courses were normalized using the following equation, where the subscripts 0, ∞ and t denote the emission ratios before the base pulse, after detergent lysis, and at an intermediate time, respectively

$$N = \frac{\left(\frac{E_{403}}{E_{460}}\right)_t - \left(\frac{E_{403}}{E_{460}}\right)_0}{\left(\frac{E_{403}}{E_{460}}\right)_\infty - \left(\frac{E_{403}}{E_{460}}\right)_0} * 100$$

NaX Jump. The vesicle suspension was prepared as described above, hydrating the lipid cake with a 0.1 mM HPTS solution (HEPES 25 mM, pH 7) and using the same buffer for gel permeation. 104 μL of the lipid suspension placed in a fluorimetric cell and diluted to 3040 μL with the same buffer solution. The total lipid concentration in the fluorimetric cell was 0.17 mM. An aliquot of solution of the ionophore (10-60 μL of the appropriate mother solution in order to obtain the desired $mol_{compound}/mol_{lipide}$ ratio) was then added to the lipid suspension and the cell was incubated at 25°C for 5 minutes. After the incubation the time course of fluorescence was recorded for 50 s (λ_{ex1}= 460nm, λ_{ex2}= 403nm, λ_{em}= 510 nm) and then 50 μL of 2 M NaX solution (with X = Cl^-, Br^-, NO_3^-, SO_4^{2-}, ClO_4^-) were rapidly added through an injector port and the fluorescence emission was recorded for 350 s. Maximal changes in dye emission were obtained by final lysis of the liposomes with detergent (40 μL of 5% aqueous Triton® X-100). Fluorescence time courses were normalized as previously described.

Acknowledgements

This work was supported by MUR-PRIN BacHoundsproject N° 2017E44A9P_005.

Keywords: chloride transport • ionophores • liposomes • Pd complexes • diphosphine ligands

References

[1] F. M. Ashcroft, *Ion Channels and Disease*. Academic Press:San Diego, **2000**.

[2] P. A. Gale, J. T, Davis, R. Quesada, *Chemical Society Reviews* **2017**, *46*, 2497-2519.

[3] H. Li, H. Valkenier, A. G. Thorne, C. M. Dias, J. A. Cooper, M. Kieffer, N. Busschaert, P. A. Gale, D. N. Sheppard, A. P. Davis, *Chem. Sci.* **2019**, *10*, 9663-9672.

[4] R. Quesada, R. Dutzler, *J. Cystic Fibrosis* **2020**, *19*, S37–S41.

[5] M. Tosolini, P. Pengo, P. Tecilla, *Current Medicinal Chemistry* **2018**, *25*, 3560-3576.

[6] P. A. Gale, R. Pérez-Tomás, R. Quesada, *Acc. Chem. Res.* **2013**, *46*, 2801-2813.

[7] A. I. Share, K. Patel, C. Nativi, E. J. Cho, O. Francesconi, N. Busschaert, P. A. Gale, S. Roelens, J. L. Sessler, *Chem. Commun.* **2016**, *52*, 7560-7563.

[8] I. Carreira-Barral, C. Rumbo, M. Mielczarek, D. Alonso-Carrillo, E. Herran, M. Pastor, A. Del Pozo, M. García-Valverde, R. Quesada, *Chem. Commun.* **2019**, *55*, 10080-10083.

[9] L. A. Jowett, E. N. W. Howe, V. Soto-Cerrato, W. Van Rossom, R. Pérez-Tomás, P. A. Gale, *Sci. Rep.* **2017**, *7*, 9397.

[10] L. Tapia, Y. Pérez, M. Bolte, J. Casas, J. Solà, R. Quesada, I. Alfonso, *Angew. Chem. Int. Ed.* **2019**, *58*, 12465-12468.

[11] N. Busschaert, I. L. Kirby, S. Young, S. J. Coles, P. N. Horton, M. E. Light, P. A. Gale, *Angew. Chem. Int. Ed.* **2012**, *51*, 4426-4430.

[12] B. A. McNally, A. V. Koulov, T. N. Lambert, B. D. Smith, J.-B. Joos, A. L. Sisson, J. P. Clare, V. Sgarlata, L. W. Judd, G. Magro, A. P. Davis, *Chem. Eur. J.* **2008**, *14*, 9599-9606.

[13] H. Valkenier, L. W. Judd, H. Li, S. Hussain, D. N. Sheppard, A. P. Davis, *J. Am. Chem. Soc.* **2014**, *136*, 12507-12512.

[14] S. J. Moore, C. J. E. Haynes, J. Gonzalez, J. L. Sutton, S. J. Brooks, M. E. Light, J. Herniman, G. J. Langley, V. Soto-Cerrato, R. Perez-Tomas, I. Marques, P. J. Costa, V. Felix, P. A. Gale, *Chem. Sci.* **2013**, *4*, 103-117.

[15] L. W. Judd, A. P. Davis, *Chem. Commun.* **2010**, *46*, 2227-2229.

[16] S. J. Edwards, I. Marques, C. M. Dias, R. A. Tromans, N. R. Lees, V. Félix, H. Valkenier, A. P. Davis, *Chem. Eur. J.* **2016**, *22*, 2004-2011.

[17] M. J. Spooner, P. A. Gale, *Chem. Commun.* **2015**, *51*, 4883-4886.

[18] H. Valkenier, C. J. E. Haynes, J. Herniman, P. A. Gale, A. P. Davis, *Chem. Sci.* **2014**, *5*, 1128-1134.

[19] N. J. Knight, E. Hernando, C. J. E. Haynes, N. Busschaert, H. J. Clarke, K. Takimoto, M. García-Valverde, J. G. Frey, R. Quesada, P. A. Gale, *Chem. Sci.* **2016**, *7*, 160-1608.,

[20] L. Fabbrizzi, A. Poggi, *Chem. Soc. Rev.* **2013**, *42*, 1681-1699.

[21] K. Yang, H. A. Kotak, C. J.E. Haynes, *Coord. Chem. Rev.* **2022**, *470*, 214705.

[22] H. Tsukube, *J. Chem. Soc., Perkin Trans. 1* **1983**, 29-34.

[23] B. J. V. Verkuijl, A. J. Minnaard, J. G. de Vries, B. L. Feringa, *J. Org. Chem.* **2009**, *74*, 6526-6533.

[24] U. Pichler, P. Scrimin, P. Tecilla, U. Tonellato, A. Veronese, M. Verzini, *Tetrahedron Lett.* **2004**, *45*, 1643-1646.

[25] A. Giannetto, F. Nastasi, F. Puntoriero, G. Bella, S. Campagna, S. Lanza, *Dalton Trans.* **2021**, *50*, 1422–1433.

[26] T. M. Fyles, C. C. Tong, *New J. Chem.* **2007**, *31*, 655-661.

[27] F.-X. Wang, J.-W. Liu, X.-Q. Hong, C.-P. Tan, L. Zhang, W.-H. Chen, P. J. Sadler, Z.-W. Mao, *CCS Chem.* **2022**, *4*, 2409–2419.

[28] A. J. Plajer, J. Zhu, P. Pröhm, F. J. Rizzuto, U. F. Keyser, D.S. Wright, *J. Am. Chem. Soc.* **2020**, *142*, 1029–1037.

[29] L.-J. Chen, X. Wu, A. M. Gilchrist, P. A. Gale, *Angew. Chem. Int. Ed.* **2022**, *[61]*, e202116355.

[30] D. Milano, B. Benedetti, M. Boccalon, A. Brugnara, E. Iengo, P. Tecilla, *Chem. Commun.* **2014**, *50*, 9157-9160.

[31] M. Tosolini, J. Avó, A. J. Parola, G. Balducci, P. Tecilla, *Eur. J. Inorg. Chem.* **2020**, 3859–3868.

[32] P. Dierkes, P. W. N. M. van Leeuwen, *J. Chem. Soc., Dalton Trans.* **1999**, 1519−1530.

[33] C. M. Donahue, S. P. McCollom, C. M. Forrest, A. V. Blake, B. J. Bellott, J. M. Keith, S. R. Daly, *Inorg. Chem.* **2015**, 54, 5646–5659.

[34] W. L. Steffen, G. J. Palenik, *Inorg. Chem.* **1976**, *15*, 2432-2439.

[35] R. J. Burt, J. Chatt, W. Hussain, G. J. Leigh, *J. Organomet. Chem.* **1979**, *182*, 203–206.

[36] M. Van Overschelde, E. Vervecken, S. G. Modha, S. Cogen, E. Van der Eycken, J. Van der Eycken, *Tetrahedron* **2009**, *65*, 6410–6415.

[37] H. Hohmann, R. Van Eldik, *Inorg. Chim. Acta* **1990**, *174*, 87-92.

[38] M. Merritt, M. Lanier, G. Deng, S. L. Regen, *J. Am. Chem. Soc.* **1998**, *120*, 8494-8501.

[39] M. Tosolini, "Transition Metal Complexes as Anion Carriers" (2018). Electronic Thesis and Dissertation Repository. http://hdl.handle.net/11368/2962375

[40] http://app.supramolecular.org/bindfit/.

[41] P. Thordarson, *Chemical Society Reviews* **2011**, *40*, 1305-1323.

[42] X. Wu, P. A. Gale, *Chem. Commun.* **2021**, *57*, 3979-3982.

[43] S. J. Moore, C. J. E. Haynes, J. González, J. L. Sutton, S. J. Brooks, M. E. Light, J. Herniman, G. J. Langley, V. Soto-Cerrato, R. Pérez-Tomás, I. Marques, P. J. Costa, V. Félix, P. A. Gale, *Chem. Sci.* **2013**, *4*, 103-117.

[44] J. S. Bang, Y. J. Kim, J. Song, J.-S. Yoo, S. Lee, M. J. Lee, H. Min, K. W. Hwang, K. H. Min, *Bioorg. Med. Chem.* **2012**, *20*, 5262–5268.

[45] S. J. Sabounchei, M. Ahmadi, Z. Nasri, *J. Coord. Chem.* **2013**, *66*, 411-423.

[46] M. A. Abukari, T. Suzuki, M. Kita, *Polyhedron* **2013**, *52*, 364-369.

[47] J. A. S. Bomfim, F. P. de Souza, C. A. L. Filgueiras, A. G. de Sousa, M. T. P Gambardella, *Polyhedron* **2003**, *22*, 1567-1632.

[48] S. Daly, M. F. Haddow, A. G. Orpen, G. T. A. Rolls, D. F. Wass, R. L. Wingad, *Organometallics* **2008,** *27*, 3196–3202